FEMS Microbiology Ecology, 96, 2020, fiaa009

doi: 10.1093/femsec/fiaa009
Advance Access Publication Date: 14 January 2020
Research Article

RESEARCH ARTICLE

Bacterial community profile after the lethal infection of *Steinernema–Xenorhabdus* pairs into soil-reared *Tenebrio molitor* larvae

Marine C. Cambon[1,2,†], Pierre Lafont[1], Marie Frayssinet[2], Anne Lanois[2], Jean-Claude Ogier[2], Sylvie Pagès[2], Nathalie Parthuisot[1], Jean-Baptiste Ferdy[1] and Sophie Gaudriault[2,*,‡]

[1]Laboratoire Evolution et Diversité Biologique, CNRS-IRD-Université Paul Sabatier, 118 route de Narbonne, 31077 Toulouse, France and [2]Laboratoire Diversité, Génome et Interactions Microorganismes Insectes, INRA-Université de Montpellier, Place Eugène Bataillon, 34095 Montpellier, France

[*]**Corresponding author:**Laboratoire Diversité, Génome et Interactions Microorganismes Insectes, INRA-Université de Montpellier, Place Eugène Bataillon, 34095 Montpellier, France. Tel: +33 467 144 812; E-mail: sophie.gaudriault@umontpellier.fr

One sentence summary: The bacterial symbiont from nematode–bacteria pairs *Steinernema–Xenorhabdus* does not dominate the bacterial community of the cadaver after lethal infection of soil-reared *Tenebrio molitor* insect larvae

Editor: Cindy Nakatsu
[†]Marine C. Cambon, http://orcid.org/0000-0001-5234-4196
[‡]Sophie Gaudriault, http://orcid.org/0000-0003-2789-4959

ABSTRACT

The host microbiota may have an impact on pathogens. This is often studied in laboratory-reared hosts but rarely in individuals whose microbiota looks like that of wild animals. In this study, we modified the gut microbiota of the insect *Tenebrio molitor* by rearing larvae in soil sampled from the field. We showed by high throughput sequencing methods that this treatment modifies the gut microbiota so that it is more diversified than that of laboratory-reared insects, and closely resembled the one of soil-dwelling insects. To describe what the entomopathogenic bacterial symbiont *Xenorhabdus* (Enterobacteriaceae), vectored by the soil-dwelling nematode *Steinernema*, might experience in natural conditions, we studied the infestation of the soil-reared *T. molitor* larvae with three *Steinernema–Xenorhabdus* pairs. We performed the infestation at 18°C, which delays the emergence of new infective juveniles (IJs), the soil-dwelling nematode forms, but which is a temperature compatible with natural infestation. We analyzed by high throughput sequencing methods the composition of the bacterial community within the insect cadavers before the first emergences of IJs. These bacterial communities were generally characterized by one or two non-symbiont taxa. Even for highly lethal *Steinernema–Xenorhabdus* pairs, the symbiont does not dominate the bacterial community within the insect cadaver.

Keywords: microbiota; *Steinernema*; *Xenorhabdus*; infection; *Tenebrio molitor*; soil-rearing

Received: 12 August 2019; **Accepted:** 13 January 2020

INTRODUCTION

In the particular context of host–pathogen interactions, it has recently been shown that the host microbiota may have a positive or a negative impact on pathogens, potentially altering the outcome of infection in different model hosts (Stecher and Hardt 2008; Caccia *et al.* 2016; Shao *et al.* 2017; Onchuru, Martinez and Kaltenpoth 2018). It is, therefore, crucial to consider the interactions between pathogens and the community of microorganisms harbored by the host during infection, to understand the factors determining the outcome of infection.

In the case of insect hosts, pathogens in their microbial environment are often studied in laboratory-reared hosts but rarely in individuals whose microbiota looks like that of wild animals. However, insects living in the natural environment have a microbiota much more diverse than that of laboratory-reared insects (Chandler *et al.* 2011; Staudacher *et al.* 2016). This diversity may be responsible for interaction with the pathogen different from what is usually observed in laboratory models.

The entomopathogenic bacterium *Xenorhabdus* (Enterobacteriaceae) is transmitted by infective juveniles (IJs) of the nematode *Steinernema*. IJs are soil-dwelling forms that carry small numbers of cells of the bacterium *Xenorhabdus* in an intestinal receptacle (Martens, Heungens and Goodrich-Blair 2003; Snyder *et al.* 2007). The IJs disperse in soil until they find a larval insect host to invade. They penetrate the insect host through natural openings, perforate the insect intestinal wall and release their *Xenorhabdus* symbionts into the hemolymph (Sicard *et al.* 2004; Snyder *et al.* 2007). The bacteria then multiply in the extracellular matrix of the host tissues, suppress the host immune system and kill the insect by septicemia (Dowds and Peters 2002; Sicard *et al.* 2004; Richards and Goodrich-Blair 2009). The nematodes utilize available resources within the insect cadaver. When nutrients become limiting, the *Steinernema* IJs specifically reassociate with *Xenorhabdus* in the insect cadaver. The symbiotic IJs then disperse into the soil in search of a new host.

During its life cycle, *Xenorhabdus* almost certainly interacts with the microbiota of both the insect host and the nematode vector. Studies of different nematode–bacterium pairs, with laboratory-reared lepidopteran hosts (*Galleria* and *Manduca*) have shown that *Xenorhabdus* spp. dominates the bacterial community within the insect cadaver 48 hours after infection (Gouge and Snyder 2006; Singh *et al.* 2014), but that it coexists with other bacteria several days after the death of the host (Isaacson and Webster 2002; Walsh and Webster 2003). Other studies have demonstrated that nematodes of the genus *Steinernema,* although historically considered monoxenic, can associate with bacteria other than *Xenorhabdus*, at least in laboratory (Walsh and Webster 2003; Gouge and Snyder 2006). However, these studies used culture-dependent methods for the isolation and identification of bacteria, potentially resulting in an underestimation of microbial diversity. The recent development of sequencing techniques allows more accurate studies of the communities of microbes associated with multicellular organisms.

In this study, we described what *Xenorhabdus* experiences when infecting hosts with a diversified gut microbiota close to that of soil-dwelling insects. In this goal, we used the insect host *Tenebrio molitor,* whose larvae are sensitive to *Steinernema* (Shapiro-Ilan, Morales-Ramos and Rojas 2016), and that can be reared in soil sampled from field (Jung *et al.* 2014). Moreover, we carried-out bioassays at temperature compatible with natural infestation.

We first showed that rearing *T. molitor* larvae in soil diversifies their gut microbiota. We then infected these insects with three *Steinernema–Xenorhabdus* pairs: *Steinernema carpocapsae* SK27–*Xenorhabdus nematophila* F1, *Steinernema feltiae* FRA44–*Xenorhabdus bovienii* FR44 and *Steinernema weiseri* 583–*X. bovienii* CS03. We then analysed by high throughput sequencing methods the composition of the bacterial community within the insect cadavers 10 days after infection, before the first emergences of IJ from the insect cadavers.

MATERIAL AND METHODS

Biological material

Tenebrio molitor larvae were provided by Micronutris (St-Orens, France) and fed with heat-sterilized bran before the experiment. As it was not possible to determine their precise developmental stage, we limited the risk of including individuals at different stages by using only larvae weighing between 20 and 100 mg.

Three nematode species of the genus *Steinernema* were used to infest *T. molitor* larvae: (i) *S. carpocapsae* SK27 associated with *X. nematophila* F1 (Sc-Xn) (Brunel *et al.* 1997), (ii) *S. feltiae* FRA44 associated with *X. bovienii* FR44 (Sf-Xb) (Emelianoff *et al.* 2008a) and (iii) *S. weiseri* 583associated with *X. bovienii* CS03 (Sw-Xb) (Mrácek, Sturhan and Reid 2003). All nematode strains had been kept for several years in the laboratory, with reamplification through the infection of *Galleria mellonella* larvae, and were stored in Ringer solution at 8°C.

Symbiont load, insect mortality and parasitic success measure

We assessed the load of *Xenorhabdus* in nematodes, by surface-sterilizing 20 IJs for 10 min in 0.4% bleach and rinsing them three times in sterile Ringer solution. IJs were ground with three 3 mm glass beads in 200 μL of Luria-Bertani (LB) broth for 10 min at 30 Hz in a TissueLyser II (Qiagen, France). The resulting suspension was plated on nutrient bromothymol blue agar (NBTA) plates (Boemare, Thaler and Lanois 1997), on which *Xenorhabdus* form blue colonies. Blue colony-forming units (CFU) were counted to estimate the number of *Xenorhabdus* bacterial cells per nematode. *Xenorhabdus* load of IJs used for the experiments was as follow: 94 ± 42 CFU/IJ for Sc, which is consistent with previous findings (Goetsch *et al.* 2006; Snyder *et al.* 2007); 3 ± 2 CFU/IJ for Sf; < 0.05 CFU/IJ for Sw. Colonies with a different morphology and color from those of *Xenorhabdus* were identified by amplifying and sequencing the 16S rRNA gene as previously described (Jiang *et al.* 2006).

Insect mortality and parasitic success of nematodes were measured by infecting 30 bran-reared *T. molitor* larvae with 50 IJs in 100 μL of Ringer solution. Parasitic success was calculated as the proportion of insect cadavers displaying IJ emergence.

Rearing of insects in soil samples

We produced hosts with a microbiota as close as possible to the naturally occurring microbiota while controlling for other insect characteristics, by acclimating laboratory-reared *T. molitor* to soil samples. We sampled soil from riverside land around Montpellier in the South of France: on the banks of the Hérault river near Causse-De-La-Selle (N43°49.884′ E003°41.222′; CDS sample, Fig. 1A) and on those of the Lez river near Montferrier-sur-Lez (N43°40.801′ E003°51.835′; MTF sample, Fig. 1A). We collected three soil subsamples from each plot. These subsamples were taken at a depth of 20 cm and were separated by a distance of

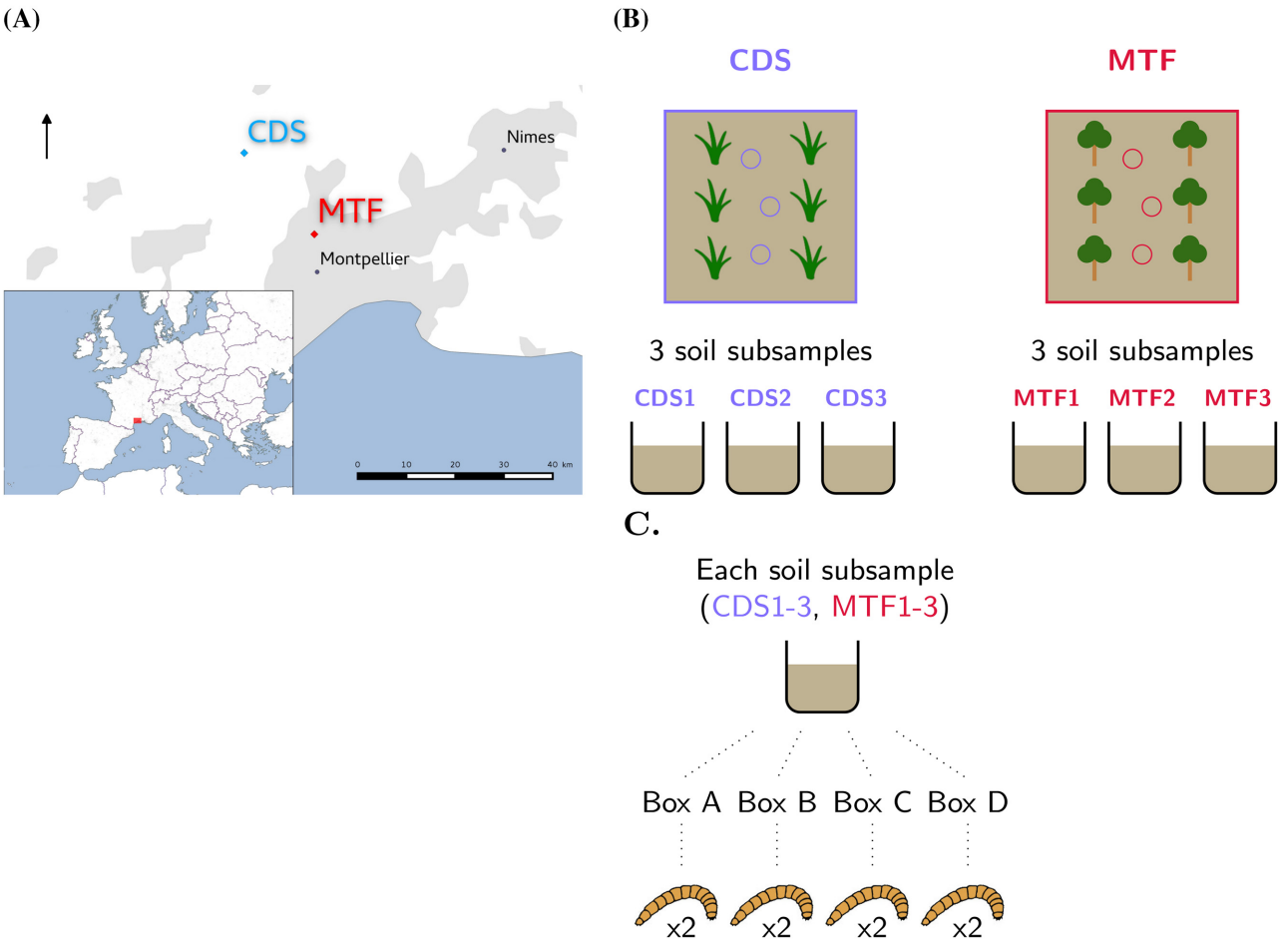

Figure 1. Experimental design for insect acclimatization in soils. **A.** Location of the two sampling sites. CDS: Causse-De-La-Selle (N43°49.884′ E003°41.222′; CDS sample); MTF: Montferrier-sur-Lez (N43°40.801′ E003°51.835′; MTF sample). **B.** At each sampling site, we obtained three soil subsamples at positions 10 m apart. **C.** Distribution of insects in soil subsamples. Each soil subsample was split into four portions, each of which was placed in a plastic box, in which it was mixed with sterilized wheat bran.

10 m. They were named CDS1, CDS2, CDS3 and MTF1, MTF2, MTF3 (Fig. 1B). Each soil subsample was split into four portions, each of which was placed in a 1 L plastic box (Fig. 1C), in which it was mixed with heat-sterilized (20 min at 121°C) wheat bran (1:3 (v/v) ratio, as previously described (Jung *et al.* 2014).

Tenebrio molitor larvae were maintained for 5 days in sterilized wheat bran mixed with soil samples at 15°C. They were then starved for 24 hours to exclude individuals that were infected with pathogens (which would have died within this 24 hours period) and to limit the risk that the DNA we extract comes from the larval alimentary bolus.

To check for the impact of soil rearing on gut microbiota composition, we reared some *T. molitor* larvae in the same conditions as other insects except that they were incubated in sterile wheat bran, with no soil mixed. Gut microbiota of these bran-reared insects should thus be close to what it was for all insects before the experiment.

To further extract DNA from insect guts, insect larvae were then washed in 70% ethanol, rinsed in water and then killed. The guts of the larvae were dissected in sterile Ringer solution (Jung *et al.* 2014). Dissection tools were sterilized with 70% ethanol between insects.

Insect infection with nematode-bacterium pairs

Soil-acclimated *T. molitor* larvae were infected by placing them in Eppendorf tubes (one insect per tube) on a filter paper soaked with 100 μL of Ringer solution containing 50 IJs.

Insects that were not infested with nematode had their gut wall artificially wounded with a pin through the anus, resulting in insect death. The wound created in this way mimicked the gut wall lesion caused by nematodes, and may have allowed some of the bacteria from the gut microbiota to colonize the insect general cavity in an opportunistic manner. The wounded insects were also placed in an Eppendorf tube on a filter paper soaked with 100 μL of Ringer solution.

All insects were then incubated at 18°C for 10 days, before the first emergences of the IJs from the insect cadavers. At the end of this period, only dead insects were retained and whole insect cadavers were subjected to metabarcoding analysis. In dead insects, the gut barrier is destroyed, the tissues macerate and the organ compartmentalization disappears. It is therefore not possible to specifically dissect the insect gut. We used sample size of 35, 59, 20 and 18 insects for wounded insects, Sc-Xn, Sf-Xb and Sw-Xb, respectively.

DNA extraction and V3-V4 marker sequencing

Dissected guts or insect cadavers were placed in an Eppendorf tube (one insect per tube), freezed for 15 min at −80°C (for whole insects only) and ground with 3 mm steel beads for 30 s at 20 Hz with a TissueLyzer (Qiagen). One hundred μL of lysis solution (Quick Extract, Bacterial DNA extraction TEBU-BIO) and 1 μL of lysozyme from the Quick Extract kit were added. Samples were incubated at room temperature for 2 days, frozen in liquid nitrogen and heated at 95°C to ensure that all the cells were lysed. DNA was prepared by the phenol–chloroform–alcohol and chloroform extraction method, and precipitated in ethanol. Negative extraction controls were included in which all the extraction steps were performed in the absence of biological material, for detection of potential reagent contamination. DNA quantity and quality were checked by spectrophotometry using Nanodrop 2000 (ThermoScientific).

For the metabarcoding tests on insect acclimatization in soil, the V3-V4 region of the 16S rRNA gene was amplified with the PCR1F_460 (5′-ACGGRAGGCAGCAG-3′) / PCR1R_460 (5′-TACCAGG GTATCTAATCCT-3′) primers (modified versions of the primers used in a previous study (Klindworth *et al.* 2012)). For the experiment on infected insects, due to the large number of samples, PCR1F_460 and PCR1R_460 primers were fused to a unique eight nucleotide tag for sample multiplexing. Some unused tag combinations were kept for the detection of potential tag switching events (see Metabarcoding data treatment). In both experiments, amplification was performed with the MTP Taq polymerase (Sigma, ref 172-5330), according to the manufacturer's protocol, with between 3 and 70 ng of DNA for each sample, and with the following amplification program: 60 s at 94°C, 30 cycles of 60 s at 94°C, 60 s at 65°C, 60 s at 72°C and a final 10 min at 72°C. Negative and positive controls were set up with water and bacterial DNA extracted from a pure culture of *X. nematophila* respectively. Polymerase chain reaction (PCR) amplicons were checked by electrophoresis in a 1% agarose gel.

Amplicons were sequenced by the GeT-Plage genomic platform at Genotoul (Toulouse, France) with Illumina MiSeq technology and a 2 × 250 bp kit. We performed technical replicates for the PCR and sequencing steps and obtained similar relative abundance of operational taxonomic units (OTUs) (Fig. S1A, Supporting Information).

Metabarcoding data treatment

Sequence data were analyzed with OBITools (Boyer *et al.* 2015). Raw paired-end reads were aligned and merged, and alignment score was calculated. Reads with low alignment scores (<50), containing unknown bases or with an unexpected size (<400 bp or > 470 bp) were removed from the dataset. After primer trimming and sample demultiplexing, sequences found only once in the dataset were also removed (Auer *et al.* 2017). Sequences were then clustered into OTUs with the Sumaclust algorithm (Mercier *et al.* 2013), using a 97% similarity threshold. In total, 2127 OTUs, corresponding to less than 0.005% of the total number of reads of the dataset, were removed (Bokulich *et al.* 2013). The remaining OTUs were assigned to a taxonomic group with RDPclassifier (Wang *et al.* 2007) and the RDPII reference database. Sequences of OTUs assigned to the genus *Xenorhabdus* where then blasted on NCBI database to distinguish *X. nematophila* and *X. bovienii* species.

For the removal of false-positives, we identified OTUs occurring in sequencing blank controls and calculated the total number of these OTUs in the dataset. These OTUs were then removed from samples if their abundance was below 3% of the total number of reads. The distribution of each OTU in unused tag combinations was also used to filter the OTUs in each sample, by assessing the deviation of OTU abundance values from this distribution (Esling, Lejzerowicz and Pawlowski 2015).

Community analysis

Analyses were performed with R version 3.5.0 (R Core Team 2018). Chao1, Shannon and Pielou indices and Bray–Curtis distance were estimated with the vegan package of R (Oksanen *et al.* 2017). Differences in alpha diversity between treatments were assessed by non parametric methods (*i.e.* Kruskal–Wallis and Wilcoxon rank sum tests). The Bray–Curtis distance matrix was represented as a tree, using the neighbor-joining algorithm as implemented in the ape package (Paradis, Claude and Strimmer 2004). Differences in bacterial community composition were assessed with PERMANOVA tests from the vegan package (Oksanen *et al.* 2017) after checking the data dispersion using betadisper function from the same package. A first model was adjusted on the complete dataset, with the explanatory variables being infection (*i.e.* infected versus wounded insects), and site (CDS versus MTF) and the interaction between infection and site. A second model was adjusted on data for infected insects only, with the explanatory variables being nematode-bacterium pair (*i.e.* Sc-Xn, Sf-Xb or Sw-Xb), and site, and the interaction between nematode–bacterium pair and site.

Bacterial quantification by quantitative PCR

The changes in abundance of *Pseudomonas* genus and Enterobacteriaceae family in the gut microbiota of soil-reared and bran-reared insects were assessed quantifying two specific markers (Table 1) using quantitative PCR (qPCR). All qPCRs were performed in triplicate, with 3 μL of reaction mixture, on a LightCycler480 machine (Roche Diagnostics), after the plate had been filled by an Echo 525 liquid handler (Labcyte). The reagent concentrations were identical in all SYBR Green I assay reactions: 1X Light-Cycler 480 SYBR Green I Master Mix (Roche Diagnostics), 500 nM each of the forward and reverse primers specific for genus *Pseudomonas* (*Pse*-16S), the Enterobacteriaceae family (Entero-*rplP*) or the *Eubacteria* kingdom (UNI16S) and DNA matrix. The DNA used was either genomic DNA (0.5 ng/μL) for Entero-*rlp* positive controls (*Escherichia coli*, *Serratia marcesens*, *Klebsiella pneumoniae*, *Salmonella typhimurium* and *Enterobacter cloacae*), *Pse*-16S positive controls (*Pseudomonas aeruginosa* and *Pseudomonas protegens*) or Entero-*rlp* and *Pse*-16S negative controls (*Stenotrophomonas*, *Acinetobacter* and *Enterococcus*) or a 1/100 dilution of insect gut DNA for metabarcoding. The qPCR conditions were 10 min at 95°C, followed by 45 cycles of 5 s at 95°C, 10 s at 62°C and 15 s at 72°C, with a final dissociation curve segment. Cycle threshold (Ct) values were determined with LightCycler 480 software. After the validation of primer specificity (13 < Ct < 37 for positive controls, Ct > 40 for negative controls), absolute quantifications were calculated by the standard curve method. Serial dilutions of standard samples consisting of genomic DNA from *E. coli* ATCC25922 for Entero-*rplP* primers and the UNI16S primers and genomic DNA from *P. aeruginosa* CIP76.110 (= ATCC27853) for the *Pse*-16S primers were prepared and used for calibration. The R^2 values for the standard curves were 0.999 for all markers. The PCR efficiencies measured on a pool of the samples subsequently quantified were 2, 1.8 and 1.9 for Pse-16S, Entero-rplP and UNI16S primers, respectively. The gene copy number (GCN) of the target gene [copies] in

Table 1. Primers and probes used for quantification by qPCR and ddPCR.

Target gene	Primer/Probe name	Sequence (5′-3′)	Amplicon size (bp)	Specificity	Reference
V3-V4 region of 16S rRNA	Pse435_F	ACTTTAAGTTGGGAGGAAGGG	251	*Pseudomonas* genus	Bergmark *et al.* (2012)
	Pse435_R	ACACAGGAAATCCACCACCC			
rplP gene	rplP-1_F	ATGTTACAACCAAAGCGTACATTACCYTGA CGCTTAACTGC	185	Enterobacteriaceae family	Takahashi *et al.* (2017)
	rplP-185_R	ACACAGGAAATTCCACCACCC			
Heme receptor encoding gene (XNC1_0073)	Xeno_R	TGGTTTCCACTTTGGTATTGATGCC	186	*Xenorhabdus* genus	this study
	Xeno_F	ATGGCGCCAATAACCGCAACTA			
	Xeno_P	HEX/CCCCTTTTGGCACGACATCA/BHQ1			
ITS	Steiner_R	GACCCTCAATTGAACATACTAACAGATA	157	*Steinernema* genus	this study
	Steiner_F	TATCAAGTCTTATCGGTGGATCACT			
	Steiner_P	6FAM/GGTCGATGAAAAACGGGGCA/BHQ1			
16S rRNA	UNI16S_F	CCATGAAGTCGGAATCGCTAG	81	Eubacteria	Vandeputte *et al.* (2017)
	UNI16S_R	GCTTGACGGGCGGTGT			

standard samples was estimated using the total amount of genomic DNA in the calibration samples [g], the size of the bacterial chromosome [bp], the number of targets per bacterial chromosome [copies], Avogadro's constant [bp mol^{-1}] and the mean weight of a double-stranded base pair (660 g mol^{-1} bp^{-1}) as follows:

Using the parameters of the curves linking and in standard samples, we then estimated the GCN of target genes in our gut samples. This estimation was possible because PCR efficiency was very close to that for standard samples.

Bacterial quantification and IJ detection by digital droplet PCR

The bacteria *Xenorhabdus* were quantified in infected insects by duplex digital droplet PCR (ddPCR) using a *Xenorhabdus*-specific primers couple targeting a region of a TonB-dependant heme-receptor encoding gene (JC Ogier, personal communication; Table 1). The nematodes were detected with a specific primers couple targeting the internal transcribed spacer (ITS) region of the ribosomal DNA (JC Ogier, personal communication; Table 1). The TaqMan probes used in ddPCR were synthesized by labeling the 5′-terminal nucleotide with the 6-carboxy-fluorescein (FAM) and HEX reporter dyes for the *Steinernema*_ITS and the *Xenorhabdus* heme receptor gene, respectively. Single ddPCR assay using EvaGreen was used with universal bacterial 16rRNA primers to quantify all bacteria in the samples. The QX200™Droplet Digital™ PCR System (Bio-Rad, Marne-la-Coquette, France) was used in this study according to the manufacturer's instructions. Briefly, for duplex assays, the ddPCR reaction mixtures (22 µl) contained: 1x ddPCR Supermix (No dUTP) (Bio-Rad, Marne-la-Coquette, France), 900 nM of each primer, 250 nM of each probe and 2 μl of DNA sample, in a final volume of 22 μl. For single EvaGreen ddPCR, the reaction mixtures were the same except for primers that were used at 100 nM each and Supermix was EvaGreen (1x) (Bio-Rad, Marne-la-Coquette, France).

Droplets were generated by the QX200 Droplet Generator AutoDG (Bio-Rad), using 20 μl of the ddPCR mixture and 70 μl droplet generation oil (Bio-Rad). The entire droplet emulsion volume (40 μl) was further loaded onto a 96-well PCR plate (Bio-Rad) and sealed in the PX1 PCR Plate Sealer (Bio-Rad). The PCR was performed in a T100 Thermal Cycler (Bio-Rad with 10 min DNA polymerase activation at 95°C, followed by 40 cycles of a two-step thermal profile of 30 s at 94°C for denaturation, and 60 s at 56°C for annealing and extension, followed by a final hold of 10 min at 98°C for droplet stabilization and cooling to 4°C. The PCR cycling conditions for the single EvaGreen ddPCR consisted of 5 min initial denaturation at 95°C, followed by 40 cycles of denaturation at 95°C for 30 s and annealing/elongation at 60°C for 1 min and final 5 min incubation at 4°C followed by 5 min at 90°C for signal stabilization. The temperature ramp rate was set to 2°C/s for both ddPCR assays, and the lid was heated to 105°C, according to the Bio-Rad recommendations. After thermal cycling, the plate containing the droplets was placed in a QX200 droplet reader (Bio-Rad, Marne-la-Coquette, France) for analyzing each individual droplet by a detector. The ddPCR data were analyzed with QuantaSoft analysis software version 1.7.4.0917 (Bio-Rad).

RESULTS

Insect acclimatization in soil

Xenorhabdus sp. being a pathogen of soil dwelling-insects, we wanted to perform infections on insects having a diversified microbiota as it is generally observed in soil-dwelling insects (Vasanthakumar *et al.* 2008; Arias-Cordero *et al.* 2012; Wang and Rozen 2017). To do so, we first tested the effect of soil acclimatization of lab-reared insects on their gut microbiota. We maintained laboratory-reared *T. molitor* larvae for a few days in either sterilized bran or sterilized bran mixed with soil samples. We sampled soil from two different riverside plots from the area around Montpellier (France): CDS and MTF (Fig. 1A). We collected three soil subsamples from each plot: CDS1, CDS2, CDS3 and MTF1, MTF2, MTF3 (Fig. 1B). The use of these six soil subsamples allowed us to compare the variability of changes in microbiota composition both within and between plots. Each sample was mixed with sterilized wheat bran and split into four, with each subsample transferred to a separate box into which larvae were placed (Fig. 1C). Bran-reared insects were incubated in sterile wheat bran alone. A first experiment of metabarcoding was performed on the gut microbiota of larvae, by targeting the V3-V4 region of the 16S rRNA gene. After cleaning, the total dataset contained 814,482 sequences, clustered into 106 OTUs. Sequencing depth for samples ranged from 6142 to 31,008 reads (mean = 15 663.12, sd = 6711.397, see samples rarefaction curves Fig. S1B, Supporting Information).

To check if incubation in soil did modify the bacterial community in insect gut microbiota, we compared the alpha diversity (Shannon index) between soil-reared and bran-reared insects. Alpha diversity of the gut microbiota increased significantly after the incubation of the insects with soil samples (Fig. 2A, soil-reared versus bran-reared: Wilcoxon rank sum test, W = 216, *P*-value = 1e-3). We also investigated the effect of soil treatments according to soil origin, by comparing the alpha diversity of CDS and MTF samples. Shannon index was significantly lower in MTF than in CDS samples (Fig. 2A; Kruskal–Wallis test, $Chi^2 = 9.6136$, *P*-value = 1e-3).

We then investigated the effect of soil treatment on insect microbiota composition. Calculation of beta-diversity between insect gut microbiota with Bray–Curtis distances (Fig. 2B) indicates that community structure differed between soil-reared insects and bran-reared insects (PERMANOVA analysis, soil-reared versus bran-reared: $R^2 = 0.19$, *P*-value = 2e-3). When comparing soil-reared insects only, soil sampling site (i.e. CDS or MTF) and subsample identity (e.g. CDS1, CDS2 or CDS3), also had a significant impact on gut community composition (PERMANOVA analysis, sampling site: $R^2 = 0.08$, *P*-value = 2e-3; subsample: $R^2 = 0.18$, *P*-value = 1e-3). Overall, our results show that soil treatment is associated with change in the community composition of the gut microbiota and that bacterial communities present in the gut differ both between sample sites and between soil subsamples.

After OTU affiliation, we observed that *Pseudomonas* is the dominant OTU in bran-reared insects (98% of the reads), but accounted for only 27 and 23% of the reads in CDS and MTF samples, respectively (Fig. 2C). Conversely, *Serratia* species, together with the *Enterobacter* group accounted for less than 1% of sequence reads in bran-reared insects, but for 35 and 43% of the reads for CDS and MTF, respectively.

Metabarcoding is not a quantitative method, but only gives semi-quantitative information (Ogier *et al.* 2019). To precisely quantify the abundance modification of the major taxa in the gut microbiota after soil rearing, we performed qPCR on a subset of 17 samples, including the five bran-reared insects and two insects for each soil subsample. We first calculated the GCN of the 16S rRNA gene in each sample, which ranged from 1e7 to 1e8 GCN per insect. Although the number of 16S rRNA gene

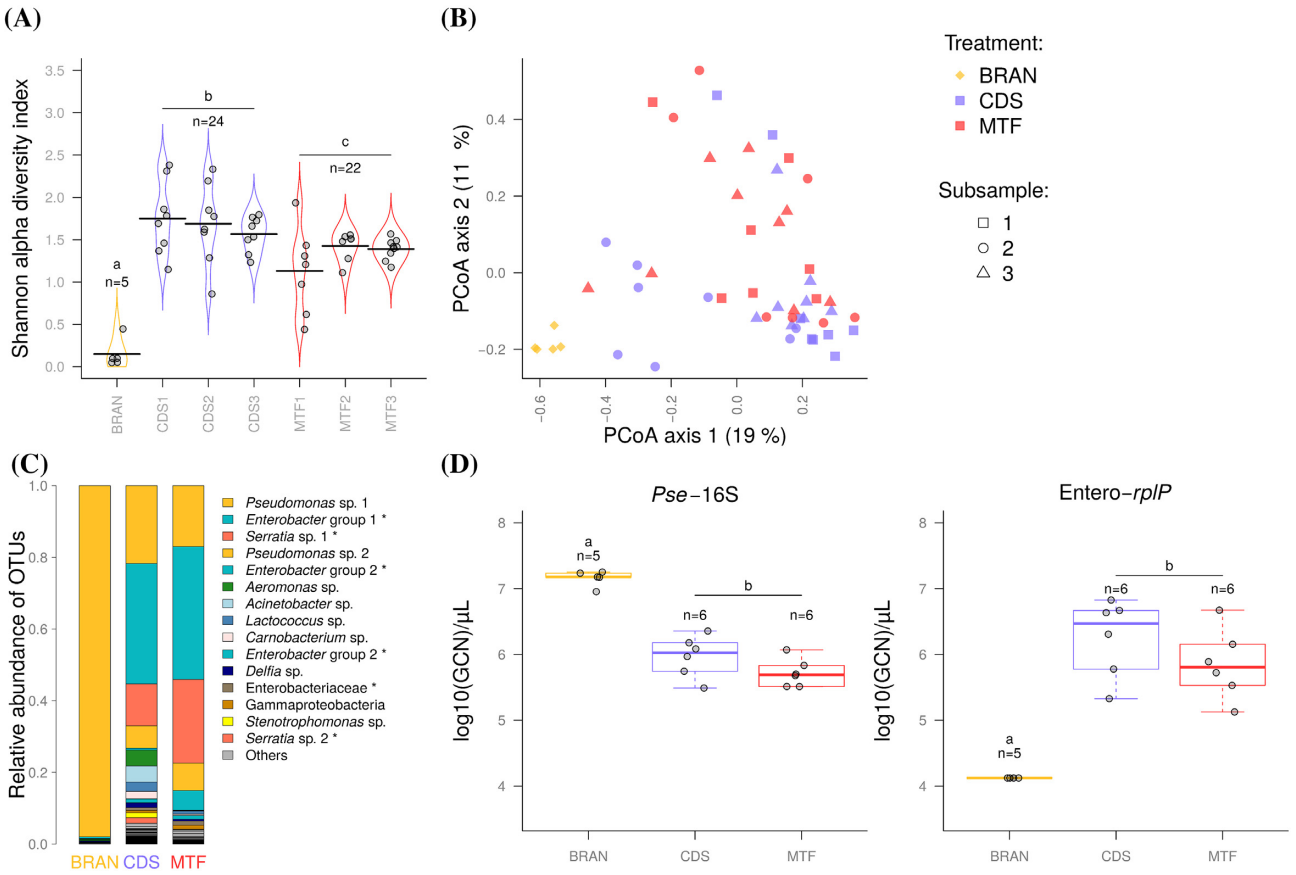

Figure 2. Influence of insect soil acclimatization on composition and structure of *T. molitor* gut microbiota. **A.** Alpha diversity of the insect gut microbiota acclimated to soils. Shannon diversity index was calculated. CDS1–3 and MTF1–3 are the subsamples from the sampling sites (three for CDS and three for MTF). BRAN samples are insects reared on sterile wheat bran. Pairwise Wilcoxon rank-sum test, CDS-MTF: *P*-value = 1e-3, SON-CDS: *P*-value = 5e-05, SON-MTF: *P*-value = 8e-05. **B.** Beta diversity of the insect gut microbiota acclimated to soils. PCoA analysis based on Bray–Curtis distance. Each dot corresponds to one insect. The percentage of variance explained by each axis is indicated in brackets. **C.** Composition of insect gut microbiota. We show here taxonomic assignments to genus level or to the lowest taxonomic level, for which the bootstrap score was < 80%. The 15 OTUs with the largest relative abundance are shown in color and the others are grouped together in the 'Others' category. OTU names followed by a star (*) belong to the Enterobacteriaceae family. **D.** Quantitative PCR on the Pseudomonas genus and the Enterobacteriaceae family present in the insect gut microbiota. GCN per µL of DNA extract was calculated for the genus Pseudomonas with the Pse-16S marker and for the Enterobacteriaceae family with the Entero-rplP marker. Pairwise Wilcoxon rank sum test with Holm *P*-value adjustment, BRAN-CDS_Pse-16S: *P*-value = 0.013, BRAN-MTF_Pse-16S: *P*-value = 0.013, MTF-CDS_Pse-16S: *P*-value = 0.18, BRAN-CDS_Entero-rplP: *P*-value = 0.016, BRAN-MTF_Entero-rplP: *P*-value = 0.016, MTF-CDS_Entero-rplP: *P*-value = 0.31. For Entero-rplP, samples from BRAN treatment had the maximum Ct value of 40, meaning that the Entero-rplP quantity was under the qPCR detection threshold.

copies varies across Eubacteria lineages, we used it as a proxy of the total number of bacteria and concluded that it was similar in our 17 samples (Kruskal–Wallis rank sum test, $Chi^2 = 2.66$, df = 2, *P*-value = 0.26). We then targeted a region of the 16S rRNA gene (4 to 7 copies per genome (Bergmark *et al.* 2012)) specific to the *Pseudomonas* genus, and a region of the *rplP* gene (one copy by genome (Takahashi *et al.* 2017)) specific to the Enterobacteriaceae family. The Pse-16S GCN in soil-reared insects was one tenth that in bran-reared insects (Pairwise Wilcoxon rank sum test with Holm *P*-value adjustment, BRAN-CDS: *P*-value = 0.013, BRAN-MTF: *P*-value = 0.013, MTF-CDS: *P*-value = 0.18, Fig. 2D). Conversely, the Entero-*rplP* GCN was 100 times higher in soil-reared insects (Pairwise Wilcoxon rank sum test with Holm *P*-value adjustment, BRAN-CDS: *P*-value = 0.016, BRAN-MTF: *P*-value = 0.016, MTF-CDS: *P*-value = 0.31, Fig. 2D). Soil acclimatization is therefore associated with a decrease in *Pseudomonas* abundance and an increase in Enterobacteriaceae abundance. Our data suggest that variation in relative abundance of the gut microbiota was associated with rearing insects in soil.

Bran-reared and soil-reared *T. molitor* larvae are sensitive to *Steinernema* nematodes at a suboptimal temperature

In the laboratory, experiments involving entomopathogenic nematodes are usually performed at a temperature allowing optimal insect infection and nematodes reproduction (e.g. 24°C in Emelianoff *et al.* (2008b)). In this study, we reduced the temperature of incubation to 18°C to be closer to natural conditions (8 to 10°C in our soil at the time of soil sampling) while staying in the range of temperatures compatible with significant mortality in laboratory (Grewal, Selvan and Gaugler 1994; Saunders and Webster 1999). At this suboptimal temperature, we first checked if bran-reared *T. molitor* larvae were sensitive to the three nematode–bacteria pairs used in our experiments, *S. carpocapsae* SK27 carrying the *X. nematophila* F1 symbiont (Sc-Xn), *S. feltiae* FRA44 carrying the *X. bovienii* FR44, symbiont (Sf-Xb) and *S. weiseri* 583 carrying the *X. bovienii* CS03 symbiont (Sw-Xb). For each tested entomopathogenic nematode (EPN) strain, we infested bran-reared *T. molitor* larvae with 50 IJs and

Table 2. Insect mortality and nematodes parasitic success for the three nematode–bacterium pairs after the infestation of bran-reared (b) or soil-reared (s) *T. molitor* larvae.

		Sc-Xn	Sf-Xb	Sw-Xb
	Nematode strain Symbiont strain	*S. carpocapsae* SK27 *X. nematophila* F1	*S. feltiae* FRA44 *X. bovienii* FR44	*S. weiseri* 583 *X. bovienii* CS03
Bran-reared *T. molitor* larvae	Host mortality Parasitic success	22/22 7/22	30/30 17/30	19/30 3/19
Soil-reared *T. molitor* larvae	Host mortality Parasitic success	48/48 21/48	–	–

Host mortality is the number of dead insects divided by the number of infected insects 10 days after infection, measured on bran-reared insects. Parasitic success is the number of insects for which IJ emergence was observed 70 days after infection.

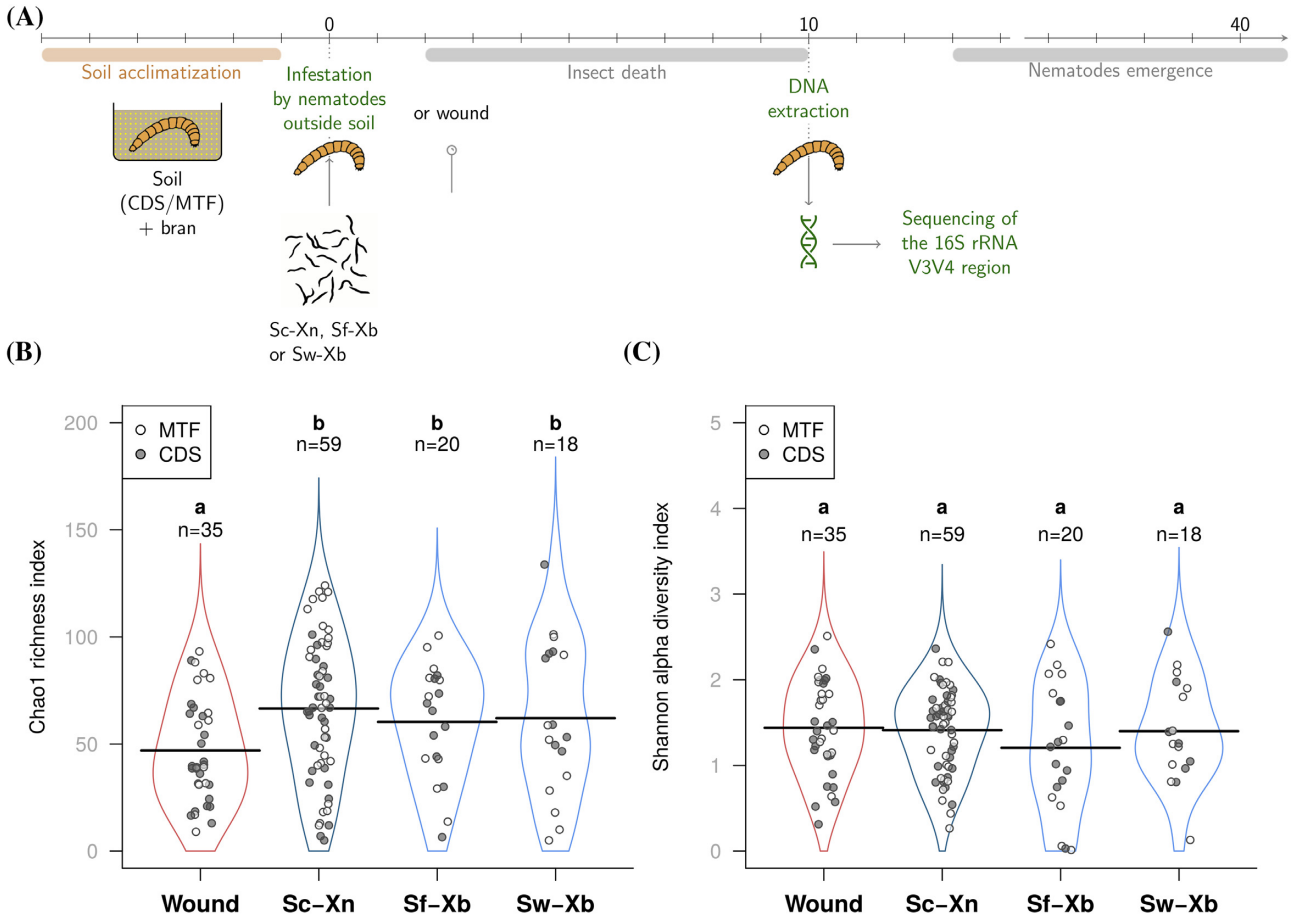

Figure 3. A. Experimental procedure for the bacterial community analysis after nematode infection. The time windows of insect death and nematodes emergences have been estimated on Sc-Xn pair. **B-C.** Comparison of alpha diversities between treatments. Each dot represents an insect and the color indicates the origin of the soil in which the insect was incubated. Sample sizes are given on the graph and letters indicate significant difference between groups. **B.** Chao1 richness index. **C.** Shannon alpha diversity index.

incubated insects at 18°C for 40 days. The insects began to die 2 days after infestation and all infected insects died within 10 days for the Sc-Xn and Sf-Xb treatments, whereas mortality was significantly lower (63%, 10 days after infection) for insects infected with Sw-Xb (Table 2, binomial generalized linar model (GLM), df = 2, *P*-value = 2.1e-05). The first IJs began to emerge about 12 days after infection and, 70 days after infestation, IJs had emerged from 32% of dead insects for the Sc-Xn/Sf-Xb treatments and 20% of dead insects for the Sw-Xb treatment (Table 2). This difference was not significant, however, possibly due to the small sample size (Binomial GLM, df = 2, *P*-value = 0.10).

We also followed the life cycle of the Sc-Xn pair on soil-reared *T. molitor* at 18°C. Insects also began to die 2 days after infestation and all infected insects died within 10 days, while nematodes started to emerge from 44% of insect cadavers, between 13 and 70 days after insect death (Table 2 and Fig. 3A). By grinding and plating on NBTA plates 20 IJs that emerged from *T. molitor* infection at 18°C, we detected the symbiont *Xenorhabdus* in 30% of the IJ samples (2–100 CFU/IJs). Moreover, 55% of the IJ samples displayed infectivity at 23°C on *G. mellonella* and produced new IJ carrying *Xenorhabdus*. Sc-Xn pair is therefore able to complete its life cycle

at 18°C on soil-reared *T. molitor* having a diversified microbiota.

Nematode infection has a small impact on bacterial diversity inside insect cadavers

To describe the bacterial community in insects after nematode–bacteria infection, we infected soil-reared *T. molitor* larvae using the three nematode-bacteria pairs Sc-Xn, Sf-Xb and Sw-Xb (Fig. 3A), and subsequently analyzed the bacterial community found in insect cadavers. The entire parasitic cycle cannot be measured since the insects are crushed for subsequent metabarcoding analysis. However, we observed that 100%, 100% and 90% of insects died after infection with Sc-Xn, Sf-Xb and Sw-Xb, respectively. Interestingly, with Sw-Xb, the infestation of soil-reared insects generates significantly higher mortality (Binomial GLM, df = 2, *P*-value = 0.03) than the one previously recorded on bran-reared insects (63% in Table 2). The difference in mortality rate suggests that bacteria from the bacteria of the microbiota coming from the soil could contribute directly or indirectly to insect death by being entomopathogenic in this condition.

In this experiment, a group of insects were not infected by nematodes. Instead, their gut wall was artificially wounded with a pin through the anus (Fig. 3A) to induce mortality and mimic the gut wall wound provoked by nematodes. This procedure resulted in an insect mortality of 70% in CDS soil and 50% in MTF soil. Mortality rates in wounded insect did not differ significantly between sites (Binomial GLM, df = 1, *P*-value = 0.12).

We sequenced the 16S rRNA V3-V4 region to describe the bacterial communities found in dead soil-reared insects (Fig. 3A). After cleaning, the total dataset contained 3827 255 sequences, clustered into 179 OTUs. The communities found in insect cadavers contained a mean of 48 ± 22, 61 ± 31, 55 ± 27 and 57 ± 31 OTUs for wound, Sc-Xn, Sf-Xb and Sw-Xb treatments, respectively. Accordingly, the Chao1 index was significantly lower in wounded insects than in insects infected with nematodes (Fig. 3B, Wilcoxon rank sum test, W = 3577.5, *P*-value = 0.02), suggesting that some of the OTUs detected were either supplied by the nematodes or a consequence of a community dynamic due to nematode infection. However, the Shannon alpha diversity index did not differ significantly between treatments (Kruskal–Wallis rank sum test, Chi^2 = 1.20, df = 3, *P*-value = 0.75), or between the wounded and infected nematodes (Fig. 3C, Wilcoxon rank sum test, W = 1608, *P*-value = 0.53). We obtained similar results in an analysis of Pielou's evenness index, which measures the similarity between the relative abundances of the different species of the community (four treatments: Kruskal–Wallis rank sum test, Chi^2 = 4.66, df = 3, *P*-value = 0.2; Wound versus infected: Wilcoxon rank sum test, W = 1414, *P*-value = 0.14). Overall, our results suggest that *Steinernema–Xenorhabdus* infections increase the number of low frequency OTUs, which appear after nematode treatment, without affecting the diversity of abundant OTUs within insect cadavers.

Infection modifies bacterial community composition but considerable inter-individual variability is observed

We analyzed the beta diversity between samples. A neighbor-joining tree based on Bray–Curtis distance did not perfectly separate wounded insects from infected insects (Fig. 4). Nematode infection had a significant impact on community composition, but it accounted for only 8% of its variance between insects (Table 3A). Soil sampling site (CDS versus MTF) accounted for 4% of the variance, and the interaction between these two variables was not significant (Table 3A).

Table 3. PERMANOVA analysis of bacterial community composition within insect cadavers.

	Df	R2	*P*-value
A.		*all insects*[1]	
Infection	1	0.08	0.001
Site	1	0.04	0.001
Infection:Site	1	0.007	0.452
B.		*infected insects only*[2]	
Nematode-bacterium pair	2	0.09	0.001
Site	1	0.04	0.002
Pair:Site	2	0.03	0.039

[1]In the first model, all insects were taken into account. We compared wounded insects to infected insects (Infection), CDS sampling site to MTF sampling site (Site) and the interaction between the two explanatory variables (Infection: Site).
[2]In the second model, only infected insects were analyzed. We compared infected insects according to the nematode-bacterium pairs (Nematode–bacteria pair), the sampling sites (Site) and the interaction of these two explanatory variables (Pair: Site).

We then compared the bacterial community composition of insects infected with the three nematode-bacterium pairs. The microbiota profile of insects infected with the same nematode–bacterium pair did not cluster together in Bray–Curtis distance trees (Fig. 4). However, nematode–bacterium pair significantly accounted for 9% of the total variance of community composition between infected insects (Table 3B). Infection thus modified the bacterial community within insect cadavers, but considerable inter-individual variability remained.

Does *Xenorhabdus* invade the bacterial community in insect cadaver?

We used the RDPII reference database for the taxonomic assignment of OTUs. Only 60% of insect larvae infected with *Steinernema–Xenorhabdus* pairs harbored a *Xenorhabdus* OTU (Fig. 4). Moreover, even in samples in which a *Xenorhabdus* OTU was detected, its relative abundance was generally low: on average, 8 ± 14% of the sample reads (Fig. 4). We validated the metabarcoding approach with a ddPCR quantification of the *Xenorhabdus* population by using a *Xenorhabdus*-specific primer couples and a ddPCR quantification of entire bacterial population by using the 16S bacterial universal marker. We then compared the relative abundance of *Xenorhabus* measured by ddPCR with the relative abundance of *Xenorhabdus* obtained by metabarcoding (Fig. 5). Doing so, we showed a correlation between those two quantities, supporting our conclusions about metabarcoding analysis (Spearman's rank correlation, rho = 0.72, *P*-value < 2.2e-16). It should be noted however that in some insects samples, no *Xenorhabdus* was detected by metabarcoding, while the amount of *Xenorhabdus* cells quantified by ddPCR was non-null (points on the x-axis in Fig. 5).

Since an absence of *Xenorhabdus* detection could be due to an absence of nematode infestation, we checked that insects contained nematodes at the time we performed the metabarcoding analysis, by quantifying the *Steinernema* population with ITS primers. In 80, 90 and 66% of the Sc-Xn, the Sf-Xb and the Sw-Xb samples, respectively, *Steinernema* was indeed detected

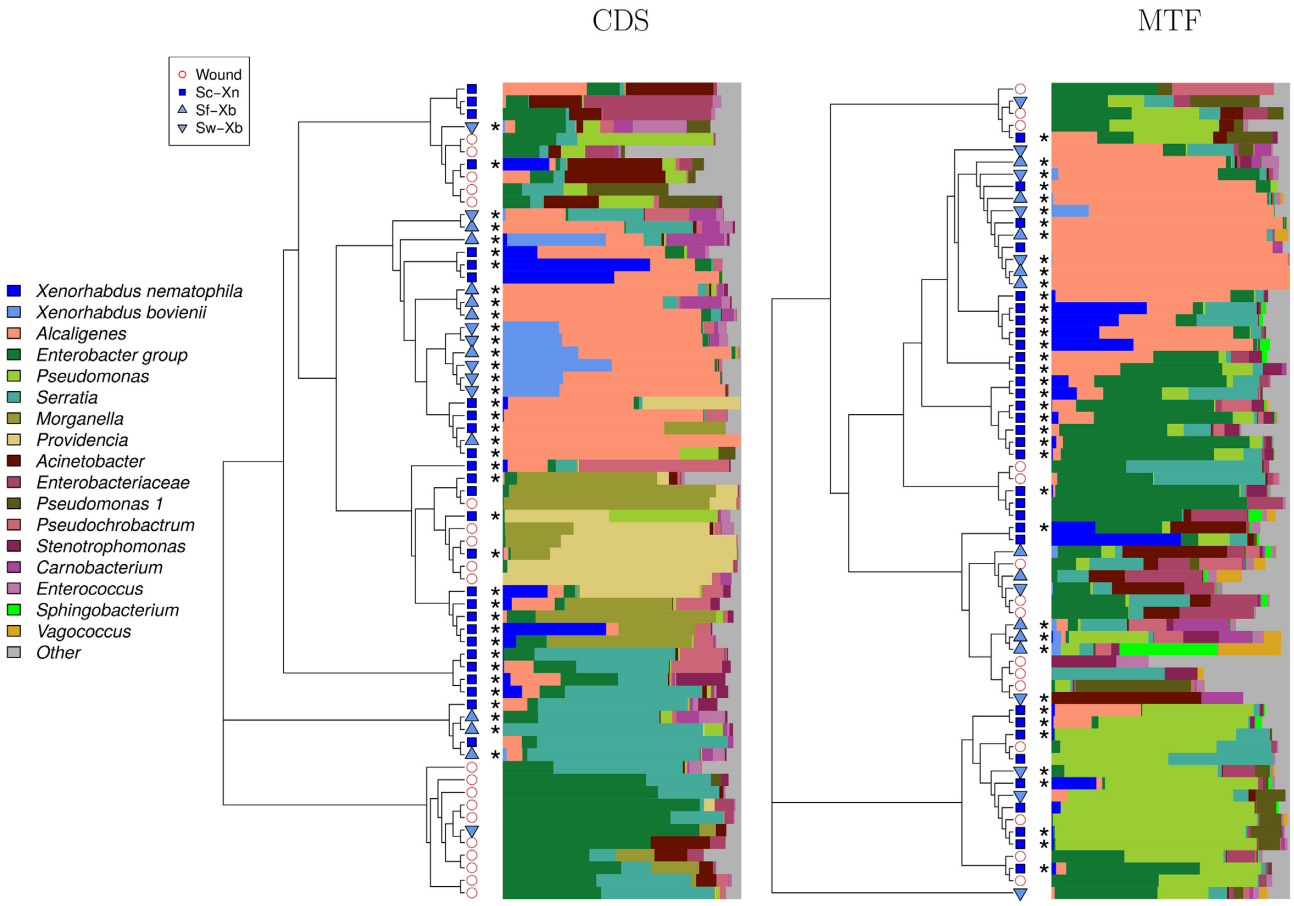

Figure 4. Beta diversity and community composition in single insect cadavers. Resemblance between bacteria communities is illustrated here by a neighbor-joining tree computed from a Bray–Curtis distance matrix (left, CDS; right, MTF). Stars indicate insects in which we detected a *Steinernema*-specific marker by ddPCR. Bars represent the relative abundance of reads matching with an OTUs in each community. On each graph, the 15 most abundant OTUs are shown in color, less frequent OTUs being grouped in the 'others' category. Greenish OTUs correspond to abundant OTUs that are potentially coming from the insect microbiota because they were found both in insects infected with nematodes and in insects that have not been in contact with nematodes. We show here taxonomic assignments (to genus level) with bootstrap scores above 80 %.

using this method (Fig. 6 and samples marked with a star on Fig. 4).

Altogether, these data suggest a surprising result. Conversely to what it is extensively described in infestation of laboratory-reared Lepidopteran insects by *Steinernema* (Isaacson and Webster 2002; Walsh and Webster 2003; Singh *et al.* 2014), *Xenorhabdus* does not dominate the bacterial community in cadavers of soil-reared *T. molitor* larvae.

Bacterial communities are dominated by one or two main OTUs

Although generally not dominated by *Xenorhabdus*, in 107 of the 132 insects tested (wounded + infected), the bacterial communities were dominated by one or two OTUs accounting for more than 40% of the sample reads. The identity of the dominant OTU varied considerably between insects and was difficult to predict from treatment (Table 3B and Fig. 4). In 32% of the infected insects, the OTUs were dominated by *Alcaligenes*, whereas OTUs from this genus were never dominant in wounded insects. We isolated an *Alcaligenes faecalis* strain from Sc and Sw nematodes, by grinding and plating surface-sterilized IJs. The 16S rRNA sequence of the isolated strain perfectly matched the V3-V4 region sequence obtained by metabarcoding on insect cadavers. It therefore seemed likely that nematodes delivered not only *Xenorhabdus*, but also *Alcaligenes*, to the insects.

Some dominant OTUs from other species were found both in insects infected with nematodes and in insects that have not been in contact with nematodes but only wounded with a pin. These OTUs cannot therefore have come from the nematode and they probably originated instead from the gut or surface insect microbiota, which has been modified or acquired during the stay in the soil. Some of these OTUs were found in both insects reared in MTF soil and insects reared in CDS soil. This was the case, in particular, for sequences from *Enterobacter* group bacteria and *Serratia*. Conversely, other dominant OTUs were specific to a site: *Morganella* and/or *Providencia* for CDS samples, and *Pseudomonas* for MTF samples (Fig. 4).

DISCUSSION

Gut microbiota communities of laboratory-reared insects, which are usually maintained on very simple media and diets, are dominated by one or two bacterial strains: *Pseudomonas* in our study, *Enterococcus* in moths (Chen *et al.* 2016; Staudacher *et al.* 2016), acetic acid bacteria or lactic acid bacteria in fruit flies (Corby-Harris *et al.* 2007, Chandler *et al.* 2011, Staubach *et al.* 2013). Following soil treatment, our *T. molitor* larvae harbored more complex community profiles, with several

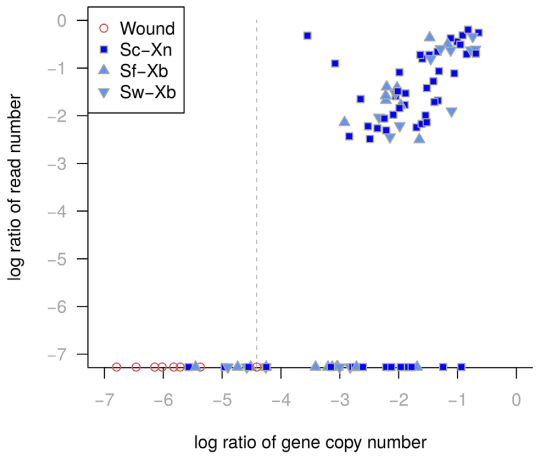

Figure 5. Validation of the metabarcoding technique through ddPCR quantification. For each insect, we represent the log ratio of the number of *Xenorhabdus* reads, over the total number of reads obtain with metabarcoding technique, against the log ratio of a *Xenorhabdus*-specific marker, over a universal 16S bacterial marker, quantified by ddPCR. We used the universal 16S bacterial marker quantification as a proxy of the total number of bacterial cells in the sample. The ddPCR ratio has been arbitrary placed on the x-axis for insects where no *Xenorhabdus* reads were obtained by metabarcoding. Dashed line represents the threshold of ddPCR quantification defined as the highest GCN of *Xenorhabdus*-specific marker we could find in uninfected insects (wound). Quantifications of *Xenorhabdus* that fell under this threshold were considered as ddPCR noise and treated as zeros.

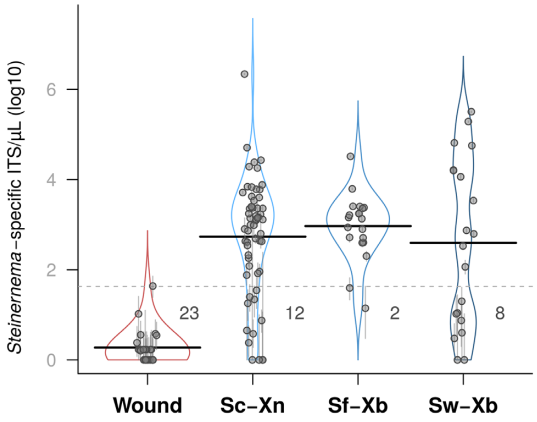

Figure 6. ddPCR quantification of a *Steinernema*-specific ITS marker in each insect. Uninfected insects (wound) were used to define a detection threshold (dashed line). Values below this threshold were considered as noise and treated as zero. The number of samples that were below this threshold is indicated for each treatment.

Enterobacteriaceae together with the *Pseudomonas* OTU that we found in bran-reared insects. Wild coleopterans, such as the forest cockchafer, *Melolontha hippocastani*, which has a soil-dwelling larval stage, have a microbiota dominated by Enterobacteriaceae, essentially a consortium of *Serratia* (Arias-Cordero *et al.* 2012), and a Shannon diversity index close to that observed here for soil-reared insects (Arias-Cordero *et al.* 2012). Other coleopterans, such as *Agrilus planipennis* and *Nicrophorus vespiloides* (Vasanthakumar *et al.* 2008; Wang and Rozen 2017) both sampled from the wild and reared on a natural diet, also have microbiota dominated by *Pseudomonas* sp., the *Enterobacter* group and *Serratia* sp.. These findings show that our protocol can be used to obtain insects with a diversified microbiota, closer to that of wild insects than to that of laboratory-reared insect.

Steinernema–Xenorhabdus pairs can infect a large spectrum of insects, but they have been studied mostly on lepidopterans. The coleopteran *T. molitor,* had seldom been studied in this context (Solomon, Paperna and Glazer 1999; Christen *et al.* 2007; Susurluk 2007; Shapiro-Ilan *et al.* 2008). We showed here that all three *Steinernema–Xenorhabdus* pairs were able to kill both bran-reared and soil-reared *T. molitor*. As previously shown in lepidopteran larvae (Bisch *et al.* 2015), the Sw-Xb pair was less pathogenic than Sc-Xn and Sf-Xb for the infection of *T. molitor* reared on sterile wheat bran. Interestingly, this difference between pathogen pairs was smaller for insects reared on soil samples: insect mortality was almost total for all pairs when soil-acclimated insects were used. This suggests that some of the bacteria present in the microbiota of soil-reared insects may opportunistically infect insects after nematodes have perforated the gut wall, contributing to insect mortality. This hypothesis is consistent with the findings of previous studies showing that infection with insect pathogens is facilitated by certain members of the host gut microbiota (Caccia *et al.* 2016).

To confirm that nematode–bacteria pairs were able to complete their life cycle when infecting soil-reared larvae, we measured the parasitic success (*i.e.* the emergence of IJs nematode from the insect cadaver) of the Sc-Xn pair when infecting soil-reared *T. molitor*. In this case, and at a suboptimal temperature of 18°C, the nematode life cycle could be completed but was delayed compared to what was classically observed on lab-reared insects. These results are consistent with previous findings on the effect of temperature on nematode life cycle (Grewal, Selvan and Gaugler 1994; Saunders and Webster 1999).

We then used metabarcoding analysis to determine the composition of the bacterial communities found in insects killed by the three *Steinernema–Xenorhabdus* pairs. These experiments were performed on soil-reared *T. molitor* 10 days after infection, a timepoint of Sc-Xn life cycle after insect death but before the first emergences of new IJs. Despite the very different levels of *Xenorhabdus* load of the three nematodes strains, the identity of the nematode–bacterium pair used for infection had no effect on alpha diversity, community evenness and a low effect on community composition. We expected the symbiont to dominate the bacterial community in the insect cadaver. Indeed, high densities of *Xenorhabdus* have been reported during the first few days of infection in Lepidopteran hosts (Isaacson and Webster 2002; Walsh and Webster 2003; Singh *et al.* 2014). However, contrary to our expectations, we found that *Xenorhabdus* did not dominate the bacterial communities in the insect cadaver 10 days after the infection of soil-reared *T. molitor* larvae. A first hypothesis to explain this surprising result may be that *Xenorhabdus* does not proliferate well in Coleopteran insects. However, *T. molitor* larvae is a usual insect for *in vivo* production of entomopathogenic nematodes (Shapiro-Ilan, Morales-Ramos and Rojas 2016). We therefore favour a second hypothesis, in which the soil-rearing of *T. molitor* larvae would be responsible for the diverse microbiota with low abundance of *Xenorhabdus*.

Xenorhabdus has a genomic potential for producing numerous anti-microbial compounds (Tobias *et al.* 2017). Organ compartmentalization disappears in the insect cadavers because of the tissue maceration. Gut-associated bacteria remaining in the gut and bacteria proliferating in the hemocoel share therefore at this timepoint the same compartment. As a result, our findings raise the question about the role of *Xenorhabdus* antimicrobials, particularly for the Sc-Xn and Sw-Xb pairs. The xenocoumacin and odilhorhabdin produced by Xn F1 have been shown to be involved in competition with bacteria within the insect cadaver (Morales-Soto and Forst 2011; Singh *et al.* 2015). The

genome of the Xb CS03 strain includes a number of specific loci potentially implicated in the inhibition of the microbial competitors, and Xb CS03 has antibacterial activity *in vitro* directed against species isolated from insects or nematodes (Bisch *et al.* 2016). The dominant OTUs from the host microbiota probably resist to the antimicrobials produced by *Xenorhabdus,* or, alternatively, these antimicrobial compounds may no longer be produced or be efficient at such late stage of infection (Isaacson and Webster 2002). An alternative explanation could also be that *Xenorhabdus* is more sensitive to nutrient depletion than other members of the microbiota in insect cadavers after ten days.

The bacterial communities in insect cadavers were mostly dominated by one or two OTUs, which is coherent with a study showing that the microbiota of decaying beetles is dominated by one bacterial family (Meyer *et al.* 2017). Some of these OTUs (*e.g. from Morganella, Providencia, Serratia* and *Enterobacter* species) likely originated from the insect microbiota, as they were found in both wounded insects with no nematode infection, and infected insects. These OTUs probably took advantage of the death of the insect provoked by the nematode–bacterium pair, as previously suggested (Isaacson and Webster 2002; Walsh and Webster 2003). The dominant OTUs from the *Enterobacter* group and from the genus *Serratia* were observed after treatments with both the soil from CDS and MTF sites. Conversely, the dominant OTUs from the genera *Morganella* and the *Providencia* were found only after treatment with CDS soil, whereas the dominant OTU from *Pseudomonas* was found mostly after treatment with MTF soil. Thus, for a given host species, *Steinernema–Xenorhabdus* pairs may encounter and potentially interact with different sets of microorganisms according to their geographical location.

In this experimental design, *Xenorhabdus* was often found together with *Alcaligenes*, which was abundant only in infected insects and was isolated from two of our nematode strains. Our results therefore strongly suggest that *Alcaligenes*, like *Xenorhabdus*, is delivered to the insect by nematode vectors. Entomopathogenic nematodes have been shown to carry several presumably non-symbiotic bacteria that they release within infected insects. Bacteria including *Acinetobacter, Pseudomonas aureofaciens, Pseudomonas fluorescens, Enterobacter agglomerans, Serratia liquefaciens, Flavobacterium sp., Providencia vermicola, Providencia rettgeri, Citrobacter freundii* and *Staphylococcus succinus* have been isolated from various *Steinernema* strains including *S. carpocapsae* and *S. feltiae* (Walsh and Webster 2003; Gouge and Snyder 2006; Somvanshi *et al.* 2006; Park *et al.* 2011; Quiroz-Castañeda *et al.* 2015; Eivazian Kary and Cand Alizadeh 2016; Eivazian Kary, Mohammadi and Girling 2017). The specific case of *A. faecalis* is interesting, as this bacterium has been isolated from different strains of *S. carpocapsae* and *S. feltiae* (Lysenko and Weiser 1974; Eivazian Kary, Mohammadi and Girling 2017), and we can now add *S. weiseri* to this list. *Alcaligenes faecalis* is thought to be non symbiotic, but these results raise questions about its role in the life cycle of *Steinernema*. In another study, the bacterial genus *Acinetobacter* displaces the *Xenorhabdus* population to dominate bacterial community present in *G. mellonella* cadavers eight days after the start of the nematode infection (Walsh and Webster 2003). It is possible that *Alcaligenes* plays a similar role in our system.

In conclusion, we show here that in our experimental conditions the bacterial communities within the insect host cadaver after EPN infestations are variable according to host individuals and geographical locations, and are not dominated, at least at one stage, by the symbiont released from the nematodes. In insect cadavers, *Xenorhabdus* species experience antagonistic interactions but also competition for resources. It was demonstrated that these interspecies competitions involve in laboratory conditions (laboratory-reared insects and elevated temperatures) both small antimicrobial molecules and bacteriocins (Morales-Soto and Forst 2011; Singh *et al.* 2015; Ciezki *et al.* 2019). Our study raised, therefore, the question of the role of these factors in bioassays close to conditions compatible with natural infestation.

SUPPLEMENTARY DATA

Supplementary data are available at FEMSEC online.

ACKNOWLEDGMENTS

We thank Lucie Zinger for help with data analysis.

FUNDING

MC obtained PhD funding from the French Ministry of Higher Education, Research and Innovation. Metabarcoding sequencing was funded by the MEM-INRA metaprogram (P10016). The work was also supported by the French Laboratory of Excellence project 'TULIP' (ANR-10-LABX-41; ANR-11-IDEX-0002-02).

Conflicts of interest. None declared.

REFERENCES

Arias-Cordero E, Ping L, Reichwald K *et al.* Comparative evaluation of the gut microbiota associated with the below- and above-ground life stages (larvae and beetles) of the Forest Cockchafer, *Melolontha hippocastani*. *PLoS One* 2012;**7**: 1–10.

Auer L, Mariadassou M, O'Donohue M *et al.* Analysis of large 16S rRNA Illumina datasets: impact of singleton read filtering on microbial community description. *Mol Ecol Resour* 2017;**17**:e122–32.

Bergmark L, Poulsen PHB, Al-Soud WA *et al.* Assessment of the specificity of Burkholderia and Pseudomonas qPCR assays for detection of these genera in soil using 454 pyrosequencing. *FEMS Microbiol Lett* 2012;**333**:77–84.

Bisch G, Ogier J-C, Médigue C *et al.* Comparative genomics between two *Xenorhabdus bovienii* strains highlights differential evolutionary scenarios within an entomopathogenic bacterial species. *Genome Biol Evol* 2016;**8**:148–60.

Bisch G, Pagès S, McMullen JG *et al. Xenorhabdus bovienii* CS03, the bacterial symbiont of the entomopathogenic nematode *Steinernema weiseri*, is a non-virulent strain against lepidopteran insects. *J Invertebr Pathol* 2015;**124**:15–22.

Boemare N, Thaler J, Lanois A. Simple bacteriological tests for phenotypic characterization of *Xenorhabdus* and *Photorhabdus* phase variants. *Symbiosis* 1997;**22**:167–75.

Bokulich NA, Subramanian S, Faith JJ *et al.* Quality-filtering vastly improves diversity estimates from Illumina amplicon sequencing. *Nat Methods* 2013;**10**:57.

Boyer F, Mercier C, Bonin A *et al.* Obitools: a unix-inspired software package for DNA metabarcoding. *Mol Ecol Resour* 2015;**16**:176–82.

Brunel B, Givaudan A, Lanois A *et al.* Fast and accurate identification of *Xenorhabdus* and *Photorhabdus* species by restriction analysis of PCR-amplified 16S rRNA genes. *Appl Environ Microbiol* 1997;**63**:574–80.

Caccia S, Di Lelio I, La Storia A *et al*. Midgut microbiota and host immunocompetence underlie *Bacillus thuringiensis* killing mechanism. *P Natl Acad Sci USA* 2016;**113**:9486–91.

Chandler JA, Lang JM, Bhatnagar S *et al*. Bacterial communities of diverse *Drosophila* species: ecological context of a host–microbe model system. *PLos Genet* 2011;**7**:e1002272.

Chen B, Teh B-S, Sun C *et al*. Biodiversity and activity of the gut microbiota across the life history of the insect herbivore Spodoptera littoralis. *Sci Rep* 2016;**6**:29505.

Christen J, Campbell J, Lewis E *et al*. Responses of the entomopathogenic nematode, *Steinernema riobrave* to its insect hosts, *Galleria mellonella* and *Tenebrio molitor*. *Parasitology* 2007;**134**:889–98.

Ciezki K, Wesener S, Jaber D *et al*. ngrA-dependent natural products are required for interspecies competition and virulence in the insect pathogenic bacterium *Xenorhabdus szentirmaii*. *Microbiology* 2019;**165**:538–53.

Corby-Harris V, Pontaroli AC, Shimkets LJ *et al*. Geographical distribution and diversity of bacteria associated with natural populations of *Drosophila melanogaster*. *Appl Environ Microbiol* 2007;**73**:3470–9.

Dowds BC, Peters A. Virulence mechanisms. In: Gaugler R (ed). *Enthomopathogenic Nematology*. New-York City, NY: CABI, 2002, 79–98.

Eivazian Kary N, Cand Alizadeh Z. Non-symbiotic association of *Citrobacter freundii* and *S taphylococcus succinus* with the entomopathogenic nematode *Steinernema feltiae*. *J Entom Soc Iran* 2016;**36**:111–9.

Eivazian Kary N, Mohammadi D, Girling R. New reports on dixenic associations between the symbionts of entomopathogenic nematodes, *Photorhabdus* and *Xenorhabdus*, and non-symbiotic bacteria. *J Crop Prot* 2017;**6**:497–511.

Emelianoff V, Chapuis E, Le Brun N *et al*. A survival-reproduction trade-off in entomopathogenic nematodes mediated by their bacterial symbionts. *Evolution* 2008b;**62**:932–42.

Emelianoff V, Le Brun N, Pagès S *et al*. Isolation and identification of entomopathogenic nematodes and their symbiotic bacteria from Hérault and Gard (Southern France). *J Invertebr Pathol* 2008a;**98**:211–7.

Esling P, Lejzerowicz F, Pawlowski J. Accurate multiplexing and filtering for high-throughput amplicon-sequencing. *Nucleic Acids Res* 2015;**43**:2513–24.

Goetsch M, Owen H, Goldman B *et al*. Analysis of the PixA inclusion body protein of *Xenorhabdus nematophila*. *J Bacteriol* 2006;**188**:2706–10.

Gouge DH, Snyder JL. Temporal association of entomopathogenic nematodes (Rhabditida: Steinernematidae and Heterorhabditidae) and bacteria. *J Invertebr Pathol* 2006;**91**:147–57.

Grewal PS, Selvan S, Gaugler R. Nematodes: niche breadth for infection, establishment, and reproduction. *J Therm Biol* 1994;**19**:245–53.

Isaacson P, Webster J. Antimicrobial activity of *Xenorhabdus* sp. RIO (Enterobacteriaceae), symbiont of the entomopathogenic nematode, *Steinernema riobrave* (Rhabditida: Steinernematidae). *J Invertebr Pathol* 2002;**79**:146–53.

Jiang H, Dong H, Zhang G *et al*. Microbial diversity in water and sediment of Lake Chaka, an athalassohaline lake in northwestern China. *Appl Environ Microbiol* 2006;**72**:3832–45.

Jung J, Heo A, Park YW *et al*. Gut microbiota of *Tenebrio molitor* and their response to environmental change. *J Microbiol Biotechnol* 2014;**24**:888–97.

Klindworth A, Pruesse E, Schweer T *et al*. Evaluation of general 16S ribosomal RNA gene PCR primers for classical and next-generation sequencing-based diversity studies. *Nucleic Acids Res* 2012;**41**:e1.

Lysenko O, Weiser J. Bacteria associated with the nematode *Neoaplectana carpocapsae* and the pathogenicity of this complex for *Galleria mellonella* larvae. *J Invertebr Pathol* 1974;**24**:332–6.

Martens EC, Heungens K, Goodrich-Blair H. Early colonization events in the mutualistic association between *Steinernema carpocapsae* nematodes and *Xenorhabdus nematophila* bacteria. *J Bacteriol* 2003;**185**:3147–54.

Mercier C, Boyer F, Bonin A *et al*. *SUMATRA and SUMACLUST: Fast and Exact Comparison and Clustering of Sequences*. 2013. http://metabarcoding.org/sumatra.2018/11/23

Meyer JM, Baskaran P, Quast C *et al*. Succession and dynamics of *Pristionchus* nematodes and their microbiome during decomposition of *Oryctes borbonicus* on La Réunion Island. *Environ Microbiol* 2017;**19**:1476–89.

Morales-Soto N, Forst SA. The xnp1 P2-like tail synthesis gene cluster encodes xenorhabdicin and is required for interspecies competition. *J Bacteriol* 2011;**193**:3624–32.

Mrácek Z, Sturhan D, Reid A. *Steinernema weiseri* n. sp.(Rhabditida, Steinernematidae), a new entomopathogenic nematode from Europe. *Syst Parasitol* 2003;**56**:37–47.

Ogier J-C, Pages S, Galan M *et al*. *rpoB*, a promising marker for analyzing the diversity of bacterial communities by amplicon sequencing. *BMC Microbiol* 2019;**19**:171.

Oksanen J, Blanchet FG, Friendly M *et al*. *vegan: Community Ecology Package*. 2017. https://CRAN.R-project.org/package = vegan.2018/11/23

Onchuru TO, Martinez A, Kaltenpoth M. The cotton stainer's gut microbiota suppresses infection of a co-transmitted trypanosomatid parasite. *Mol Ecol* 2018;**27**:3408–19.

Paradis E, Claude J, Strimmer K. APE: analyses of phylogenetics and evolution in R language. *Bioinformatics* 2004;**20**:289–90.

Park HW, Kim YO, Ha J-S *et al*. Effects of associated bacteria on the pathogenicity and reproduction of the insect-parasitic nematode *Rhabditis blumi* (Nematoda: Rhabditida). *Can J Microbiol* 2011;**57**:750–8.

Quiroz-Castañeda RE, Mendoza-Mejía A, Obregón-Barboza V *et al*. Identification of a new *Alcaligenes faecalis* strain MOR02 and assessment of its toxicity and pathogenicity to insects. *Biomed Res Int* 2015;**2015**:570243.

R Core Team. *R: A Language and Environment for Statistical Computing*. 2018. https://www.R-project.org/.2018/11/23

Richards GR, Goodrich-Blair H. Masters of conquest and pillage: *Xenorhabdus nematophila* global regulators control transitions from virulence to nutrient acquisition. *Cell Microbiol* 2009;**11**:1025–33.

Saunders J, Webster J. Temperature effects on *Heterorhabditis megidis* and *Steinernema carpocapsae* infectivity to *Galleria mellonella*. *J Nematol* 1999;**31**:299.

Shao Y, Chen B, Sun C *et al*. Symbiont-derived antimicrobials contribute to the control of the lepidopteran gut microbiota. *Cell Chem Biol* 2017;**24**:66–75.

Shapiro-Ilan D, Rojas MG, Morales-Ramos JA *et al*. Effects of host nutrition on virulence and fitness of entomopathogenic nematodes: lipid-and protein-based supplements in *Tenebrio molitor* diets. *J Nematol* 2008;**40**:13.

Shapiro-Ilan DI, Morales-Ramos JA, Rojas MG. In in vivo production of entomopathogenic nematodes. In: Glare TR, Moran-Diez ME (eds). *Microbial-based Biopesticides: Methods and Protocols*. New-York: Springer, 2016, 137–58.

Sicard M, Brugirard-Ricaud K, Pagès S *et al*. Stages of infection during the tripartite interaction between *Xenorhabdus*

nematophila, its nematode vector, and insect hosts. *Appl Environ Microbiol* 2004;**70**:6473–80.

Singh S, Orr D, Divinagracia E *et al.* Role of secondary metabolites in establishment of the mutualistic partnership between *Xenorhabdus nematophila* and the entomopathogenic nematode *Steinernema carpocapsae*. *Appl Environ Microbiol* 2015;**81**:754–64.

Singh S, Reese JM, Casanova-Torres ÁM *et al.* Microbial population dynamics in the hemolymph of *Manduca sexta* infected with *Xenorhabdus nematophila* and the entomopathogenic nematode *Steinernema carpocapsae*. *Appl Environ Microbiol* 2014;**80**:4277–85.

Snyder H, Stock SP, Kim S-K *et al.* New insights into the colonization and release processes of *Xenorhabdus nematophila* and the morphology and ultrastructure of the bacterial receptacle of its nematode host, *Steinernema carpocapsae*. *Appl Environ Microbiol* 2007;**73**:5338–46.

Solomon A, Paperna I, Glazer I. Desiccation survival of the entomopathogenic nematode *Steinernema feltiae*: induction of anhydrobiosis. *Nematology* 1999;**1**:61–68.

Somvanshi VS, Lang E, Sträubler B *et al.* *Providencia vermicola* sp. nov., isolated from infective juveniles of the entomopathogenic nematode *Steinernema thermophilum*. *Int J Syst Evol Microbiol* 2006;**56**:629–33.

Staubach F, Baines JF, Künzel S *et al.* Host species and environmental effects on bacterial communities associated with *Drosophila* in the laboratory and in the natural environment. *PLoS One* 2013;**8**:e70749.

Staudacher H, Kaltenpoth M, Breeuwer JAJ *et al.* Variability of bacterial communities in the moth *Heliothis virescens* indicates transient association with the host. *PLoS One* 2016;**11**:1–21.

Stecher B, Hardt W-D. The role of microbiota in infectious disease. *Trends Microbiol* 2008;**16**:107–14.

Susurluk A. Effectiveness of the entomopathogenic nematodes *Heterorhabditis bacteriophora* and *Steinernema feltiae* against *Tenebrio molitor* (Yellow Mealworm) larvae in different soil types at different temperatures. *Turkish Journal of Biology* 2007;**30**:199–205.

Takahashi H, Saito R, Miya S *et al.* Development of quantitative real-time PCR for detection and enumeration of Enterobacteriaceae. *Int J Food Microbiol* 2017;**246**:92–97.

Tobias NJ, Wolff H, Djahanschiri B *et al.* Natural product diversity associated with the nematode symbionts *Photorhabdus* and *Xenorhabdus*. *Nat Microbiol* 2017;**2**:1676.

Vandeputte D, Kathagen G, D'hoe K *et al.* Quantitative microbiome profiling links gut community variation to microbial load. *Nature* 2017;**551**:507–11.

Vasanthakumar A, Handelsman J, Schloss PD *et al.* Gut microbiota of an invasive subcortical beetle, *Agrilus planipennis* Fairmaire, across various life stages. *Environ Entomol* 2008;**37**:1344–53.

Walsh KT, Webster JM. Interaction of microbial populations in *Steinernema* (Steinernematidae, Nematoda) infected *Galleria mellonella* larvae. *J Invertebr Pathol* 2003;**83**:118–26.

Wang Q, Garrity GM, Tiedje JM *et al.* Naive Bayesian classifier for rapid assignment of rRNA sequences into the new bacterial taxonomy. *Appl Environ Microbiol* 2007;**73**:5261–7.

Wang Y, Rozen DE. Gut microbiota colonization and transmission in the burying beetle Nicrophorus vespilloides throughout development. *Appl Environ Microbiol* 2017;**83**:e03250–16.